

UCSF

UC San Francisco Previously Published Works

Title

Gene Expression Profiling of Transporters in the Solute Carrier and ATP-Binding Cassette Superfamilies in Human Eye Substructures

Permalink

<https://escholarship.org/uc/item/2q42h8r5>

Journal

Molecular Pharmaceutics, 10(2)

ISSN

1543-8384

Authors

Dahlin, Amber
Geier, Ethan
Stocker, Sophie L
[et al.](#)

Publication Date

2013-02-04

DOI

10.1021/mp300429e

Peer reviewed



Published in final edited form as:

Mol Pharm. 2013 February 4; 10(2): 650–663. doi:10.1021/mp300429e.

Gene Expression Profiling of Transporters in the Solute Carrier and ATP-Binding Cassette Superfamilies in Human Eye Substructures

Amber Dahlin^{1,2,^}, Ethan Geier^{1,^}, Sophie L. Stocker¹, Cheryl D. Cropp¹, Elena Grigorenko³, Michele Bloomer⁴, Julie Siegenthaler⁵, Lu Xu¹, Anthony S. Basile⁶, Diane D-S. Tang-Liu⁶, and Kathy Giacomini^{1,*}

¹Department of Bioengineering and Therapeutic Science, University of California, San Francisco, San Francisco, CA USA

³Life Technologies, Woburn, MA USA

⁴Department of Ophthalmology, University of California San Francisco, San Francisco, CA USA

⁵Department of Neurology, University of California San Francisco, San Francisco, CA USA

⁶Allergan, Inc. Irvine, CA USA

Abstract

The barrier epithelia of the cornea and retina control drug and nutrient access to various compartments of the human eye. While ocular transporters are likely to play a critical role in homeostasis and drug delivery, little is known about their expression, localization and function. In this study, the mRNA expression levels of 445 transporters, metabolic enzymes, transcription factors and nuclear receptors were profiled in five regions of the human eye: cornea, iris, ciliary body, choroid and retina. Through RNA expression profiling and immunohistochemistry, several transporters were identified as putative targets for drug transport in ocular tissues. Our analysis identified *SLC22A7* (OAT2), a carrier for the anti-viral drug, acyclovir, in the corneal epithelium, in addition to *ABCG2* (BCRP), an important xenobiotic efflux pump, in retinal nerve fibers and the retinal pigment epithelium. Collectively, our results provide an understanding of the

*Correspondence: Professor Kathleen Giacomini, Ph.D., Department of Bioengineering and Therapeutic Science, University of California, San Francisco, Rock Hall, 1550 4th Street, San Francisco, CA 94158, Phone: +1 415 476 1936, Fax: +1 415 514 4361, kathy.giacomini@ucsf.edu.

²Current address: Channing Division of Network Medicine, Brigham and Women's Hospital and Harvard Medical School, Boston, MA USA

[^]Equal contribution

SUPPLEMENTAL MATERIAL: This file contains four supplemental tables and three figures. The supplemental tables provide a detailed description of the clinical demographics of the donors who provided the eye tissues used in expression profiling experiments, details of the experimental methods and results of differential expression profiling of all array genes, as described in the text. The demographic characteristics of the eye donors are provided in S1. A comprehensive list of the genes, and their associated PCR primers used in the qPCR analysis, are provided in Table S2. Table S3 shows the results of differential expression analysis of array genes from the five eye regions vs. the human kidney, which served as the reference tissue. Table S4 provides a comparison of four transporter genes evaluated by IHC in various ocular disease states as reported in the online databases PubMed, OMIM and NEIBank. Supplemental figures S1 and S2 contain the results of hierarchical cluster analysis (S1) of expression data, and network profiling through Ingenuity Pathway Analysis (S2), respectively. Figure S3 depicts BCRP-specific IHC in the retina. These figures are described in the Results section of the text. This material is available free of charge via the Internet at <http://pubs.acs.org>.

transporters that serve to maintain ocular homeostasis and which may be potential targets for drug delivery to deep compartments of the eye.

Keywords

expression profiling; open array; gene expression; eye; cornea; retina; protein expression; transporters; acyclovir; OAT2; BCRP; OCT3

Introduction

Despite its apparent physical availability, the eye presents significant barriers to pharmacotherapeutic access, which is primarily due to the structure and function of two tissues at opposite ends of the eye: the cornea and retina. The primary physiological role of the cornea is to transmit and refract light to the retina, and to serve as a protective barrier to underlying ocular tissues. In order to provide optimal visual clarity, the cornea must be transparent; therefore, it is avascular with carefully structured cell layers [1]. The structure of the cornea consists of epithelial and endothelial cell layers separated by a collagen matrix (stroma). The corneal epithelium consists of multiple cell layers bound by tight junctions. This layer contributes to the barrier functions of the cornea by providing an osmotic gradient and limiting xenobiotic penetration into ocular compartments [2, 3]. In contrast, the retina is a highly vascularized tissue at the posterior pole of the eye. The blood-retinal barrier is composed of retinal capillaries and cells of the retinal pigment epithelium (RPE), and limits the exchange of solutes, such as nutrients and drugs, between the retina and systemic circulation. The cornea and retina represent highly specialized structures in the eye with important physiological roles, and influence the development and treatment of ocular diseases.

Because of the accessibility of the ocular surface, topical administration is the major route for administration of ophthalmics [4, 5]. To reach the anterior chamber or deeper ocular structures, topically applied ophthalmics must first be absorbed from the lacrimal fluid through the cornea. The permeation of some ophthalmic agents across ocular barrier tissues, such as the cornea, may occur through passive diffusion. However, the physicochemical properties of many ocular therapeutics necessitate active or facilitated conveyance of these compounds across membrane barriers by membrane transporter proteins [4, 6, 7]. Membrane transporters are of significant pharmacological and physiological importance due to their roles as major determinants of the absorption, distribution and elimination of numerous exogenous and endogenous substances. To date, two major superfamilies of transporters have been identified in the human genome. These are the SoLute Carrier Superfamily (SLC), consisting of 55 families and at least 362 transporter genes coding for proteins that function primarily as facilitated influx pumps [8], and the ATP Binding Cassette Superfamily (ABC), which includes seven families and 48 members, most of which are active efflux pumps driven by ATP hydrolysis [9, 10]. Given the importance of transporters as permeability barriers and selective carriers for nutrients, xenobiotics and clinically relevant drugs, a number of studies have explored their expression levels and cellular localization in tissues involved in drug absorption, distribution, metabolism and elimination

(ADME) [9, 11-18]. Transporter expression has also been evaluated in organs that are protected by blood-tissue barriers, such as the brain and testes [19-25]. This expression profiling of transporter mRNA and protein in various tissues has contributed greatly to our understanding of the molecular processes that govern drug absorption across epithelial and endothelial barriers.

Transporters expressed in the corneal epithelium and blood-retinal barriers play essential roles in mediating the absorption of drugs, other xenobiotics and nutrients into the anterior and posterior chambers of the eye [7, 26]. Despite their importance in ocular pharmacology, few studies have characterized transporter mRNA and/or protein expression, and none have evaluated the global expression levels of transporters in human ocular tissues [27-31]. Expression levels of 21 transporters in the human cornea, iris-ciliary body, and retina/choroid tissues have been assessed by semi-quantitative PCR [30], leading to the identification of several highly expressed transporters, including the organic cation transporter, OCT1, the oligopeptide transporter, PEPT2, the novel organic cation transporter, OCTN1, and the multi-drug resistance protein efflux pump, MRP1 in the eye [30]. A more recent study profiled the mRNA and protein expression of several ABC transporters, including MRP1, MRP2, MRP3, MRP4, MRP5, MRP6, P-glycoprotein and the breast cancer resistance protein (BCRP) in the developing RPE derived from human embryonic stem cells, and showed that expression of these genes is comparable to that of the human RPE cell line, ARPE-19 [31]. Although these studies provided important information on the localization and expression of a small number of pharmacologically-relevant transporters in ocular tissues, the balance of SLC and ABC transporters in the eye remain uncharacterized.

To better understand the location and expression of the greater number of transporters in ocular tissues, we applied expression profiling utilizing array-based methods. A high-throughput, semi-quantitative real-time PCR (qPCR) OpenArray® method was used in this study to profile over 400 transporters and other ADME-related genes in human ocular tissues. Immunohistochemistry and cell-based transport assays were subsequently used to localize and functionally characterize those transporters that could serve as drug and disease targets in the human eye. Most of the analyses were focused on 30 transporters of interest to the U.S. Food and Drug Administration and drug developers [32] and are referred to as TransPortal transporters (<http://bts.ucsf.edu/fdatransportal>) (Table 2). Although five ocular tissues were studied, particular emphasis was placed on the cornea and retina, which constitute major barriers to drug delivery in the eye. In this study, we profile the expression of ocular drug transporters and selectively characterize the roles of organic anion transporters that influence drug disposition in the human eye. This study establishes the identity and localization of many drug transporters within the human eye, including the organic anion transporter (OAT2), OCT3, MRP4 and BCRP. While some of these transporters may prevent the accumulation of ophthalmics within ocular compartments, others may, based on their location and function, act as conduits for accessing tissues deep within the eye.

Materials and Methods

Tissue Acquisition

Whole human eyes (orbs) from donors with no prior medical history of eye disease(s) were used for profiling transporter gene expression. Nine orbs from five individuals were procured from the National Disease Research Interchange (Philadelphia, PA), the San Diego Eye Bank (San Diego, CA) and the department of Ophthalmology at UCSF (San Francisco, CA). Six orbs from three individuals were used for gene expression profiling and three orbs from two individuals were utilized for immunohistochemistry alone. Donor demographics and medical history are provided in Supplemental Table S1. For comparative expression profiling of non-ocular tissue, normal human liver and kidney tissue were commercially obtained (Asterand, Detroit, MI). All tissues were acquired in accordance with UCSF Institutional Review Board and ethics committee guidelines (IRB number 11-06153).

Eye Dissection

Orbs were procured from donors no more than four hours postmortem in order to limit RNA and tissue degradation. Intact orbs were enucleated and placed immediately into RNA-Later Solution (Life Technologies, Grand Island, NY) for up to 48 hours at 4°C prior to dissection and processing. All subsequent tissue handling and dissection steps were performed under RNase-free conditions. For fine dissection, the orbs were rinsed in cold, RNase-free saline and kept in sterile tissue culture dishes on ice. The orbs were bisected transversely into two hemispheres, consisting of the anterior and posterior regions, respectively. The cornea, lens, iris and ciliary body were separated from the anterior hemisphere under a dissecting microscope. The retina was removed from the choroid, which was subsequently dissected from the sclera. The isolated cornea, retina, choroid, iris and ciliary body of both orbs from a single donor were placed in sterile plastic tubes containing TRIzol Reagent (1 mL/100 mg, Invitrogen, Carlsbad, CA), placed on ice and homogenized. The homogenates were stored at -80°C until RNA extraction was performed.

RNA Extraction and Reverse Transcriptase PCR

Total RNA was extracted from the eye (n=15), liver (n=60), and kidney (n=60) tissue homogenates using TRIzol Reagent and RNeasy Plus Micro Kit (Qiagen, Valencia, CA), according to the kit instructions. After separation of the organic and aqueous phases by centrifugation, total RNA was isolated from the aqueous phase using an RNeasy Plus Micro Kit. After isolation, RNA samples were stored at -80°C. Total RNA (2 µg) was reverse transcribed using the High Capacity Reverse Transcriptase kit (Life Technologies, Grand Island, NY) with random hexamer primers, followed by ExoI (GE Healthcare, Pittsburgh, PA) treatment at 37°C for 1 h. The resulting cDNA samples were stored at -80°C.

Real-time PCR

High-throughput, semi-quantitative real-time PCR was performed using a customized platform, OpenArray® system (Life Technologies, Inc, Grand Island, NY). The OpenArray® technology is based on a stainless steel “nanoplate” the size of a microscope slide that has been photolithographically patterned and etched to form a rectilinear array of

3072 × 320 μm diameter holes, each holding 33 nL. Samples were profiled on custom OpenArray® plates containing 448 pre-validated real-time SYBR Green qPCR assays. cDNA at a concentration of 108 ng/μL and SYBR Green qPCR reagent (Fast Start DNA SYBR Green kit, Roche, CA) were dispensed into an OpenArray® plate. Six cDNA samples were tested simultaneously per plate, with up to 3 plates processed per qPCR run. Real-time PCR occurred in a computer-controlled imaging thermal cycler where 9216 PCR amplifications and dissociation curves were implemented in less than four hours. The genes analyzed and the PCR primers used are listed in Table S2. Post-acquisition data processing generated fluorescence amplification and melt curves for each through-hole in the array, from which cycle threshold (C_T) and melt temperature (T_m) were computed and used for further data analysis. The relative expression of each gene in the different tissues was calculated by the C_T comparative expression method [33]. The C_T values for all the genes in each sample were calculated by subtracting the mean C_T values for three housekeeping genes (GAPDH, β -Actin, and $\beta 2$ microglobulin) from the C_T for each target gene. The relative quantity (RQ) of each gene was then determined by calculating the 2^{-C_T} value. To determine the fold change in gene expression relative to a reference tissue, the \log_2 -transformed RQ values from each tissue were compared to each other.

Statistical Analysis of Array Data

All statistical analyses were conducted using the R version 2.14.0 [34] and Bioconductor [35]. software packages. The normalized, \log_2 transformed RQ values for all samples were compared against the sample mean to compute the \log_2 ratios for each sample. The differences across sample means were evaluated using Welch's t-test. To compare gene expression patterns across samples and genes, hierarchical cluster analysis was performed using Pearson correlation distance metric and average linkage, using the Bioconductor packages *HTqPCR* and *made4* [35]. For feature selection and identification of differentially-expressed genes, the data were fitted using a linear model. The significance of the estimates returned by the fitted model were determined using an empirical Bayes moderated t-statistics test using the Bioconductor package *limma* [35].

Network Analysis

Ingenuity Pathway Analysis (IPA) is an internet-accessible database that applies known interactions among genes and curated molecular pathways (<http://www.ingenuity.com>) to gene expression data [33]. A data set containing TransPortal gene identifiers and corresponding expression values was uploaded into the IPA application and a \log_2 ratio cutoff of 1.5 was applied to identify molecules with significantly differentially regulated expression patterns. The IPA software then annotated the genes according to their curated molecular functions. Right-tailed Fishers exact test was used to calculate a P value to determine the probability that each biological function and/or disease assigned to that network is due to chance alone. The top-ranked TransPortal gene networks (based on P values) were merged with the IPA-curated HSK networks generated from the IPA database of curated pathways. The hub genes within the networks (represented as symbols), and their relationships to other genes within the network (edges) were then evaluated.

Immunohistochemistry

For immunohistochemistry (IHC), dissected eye subregions were fixed in 10% neutral buffered formalin for 48 hours, and then placed in 70% ethanol. Fixed tissues were sectioned, embedded in paraffin and mounted onto glass slides. The sections were deparaffinized in xylene and rehydrated in a graded ethanol series, followed by antigen retrieval and incubation in 0.3% hydrogen peroxide to block endogenous peroxidase activity. For the remaining IHC steps, the ABC Universal Elite Kit was used according to the manufacturer's instructions (Vector Labs, Burlingame, CA). To block nonspecific antibody binding, sections were treated with 3% normal horse serum in phosphate-buffered saline (PBS) at pH 7.4 and then incubated overnight at 4°C. with the primary antibodies listed in Table 1.

Negative control sections were treated with IgG alone or with the primary antibody omitted. Antibody specificity was determined by incubating primary antibody with a 10-fold excess of purified recombinant target protein overnight at 4°C. Tissue was then incubated with the pre-absorbed primary antibody as described above. Following primary antibody incubation, the sections were washed three times in PBS and incubated with the Universal secondary antibody for 20 minutes. Sections were washed, incubated with the Universal ABC Reagent and developed with ImmPACT NovaRed Substrate (Vector Labs, Burlingame, CA) according to the manufacturer's instructions. Developed slides were dehydrated in ethanol, coverslipped and evaluated for specific IHC signals at 20X and 40X magnification (Nikon Eclipse microscope, Nikon DS-Fi1 digital camera). An eye pathologist in the Department of Ophthalmology at the University of California, San Francisco, reviewed all slides. The image files were digitally resized using Adobe Photoshop software suite (Adobe Systems Inc., CA).

Acyclovir Transport Assay

Transport studies were performed as previously described [36]. Briefly, HEK293 cells were transiently transfected with 1 µg of OAT1, OAT2, OAT3, OAT4 or empty vector (pcDNA5/FRT) and 3 µL of Lipofectamine 2000 (Invitrogen, CA) in each well according to the manufacturer's protocol. Cells were seeded at a density of 34×10^5 cells per well in poly-D-lysine-coated 24-well plates (Becton Dickinson Biosciences, San Jose, CA) and grown overnight. Uptake assays were conducted 18 to 24 h after transient transfection by incubating the cells for 2 or 5 minutes in 0.3 mL of pre-warmed buffer containing either [³H]acyclovir (25 nM) or [³H]p-aminohippurate (PAH, 70 nM) (American Radiolabeled Chemicals, St Louis, MO) in the presence or absence of 10 µM nitrobenzylthioinosine to inhibit nonspecific nucleoside transporter mediated uptake. The reaction was terminated by washing with ice-cold Na⁺ free buffer and cells lysed in 0.1N NaOH/0.1% SDS w/v buffer. Acyclovir and PAH were quantified by liquid scintillation counting, and the amounts taken up normalized to total protein per well. The kinetics (K_m and V_{max}) of acyclovir uptake by hOAT2 were determined at 2 minutes as described above using different concentrations of [³H]acyclovir (25 - 600 µM). The data were fitted to a Michaelis-Menten curve by non-linear regression using GraphPad Prism® 4 Software (La Jolla, CA).

Results

Global expression profile of array genes in the human eye

A custom OpenArray® was designed to detect expression of 401 SLC and ABC superfamily transporters, 17 Phase I and Phase II metabolic enzymes, 20 nuclear receptors and transcription factors, seven additional enzymes and receptors relevant to drug metabolism, and three housekeeping genes (n=448 genes; Table S2). Of the 448 genes on the custom array, 435 genes (97%) were detected in at least one eye region. The cornea and retina had higher median array gene expression levels than all other tissues, with comparable gene expression ranges (Figure 1A, boxplot). To detect groups of genes with similar expression patterns, unsupervised hierarchical clustering of Pearson-correlated expression values was performed (Figure S1). Three-hundred and sixty-two genes with variable expression levels across all eye regions ($SD > 0$) were clustered on the basis of the similarity of their expression profiles (Figure S1A). This analysis identified unique sets of genes with correlated expression patterns (clusters) present within the five ocular tissues (Figure S1A). The cornea and retina contained gene clusters with the highest expression levels, which also appeared to be differentially expressed (Figure S1A and S1B). Differential expression analysis was performed to identify genes and clusters with statistically significant differences in their ocular expression patterns (Table S3). Those genes with the most significant differential expression levels (ranked by false discovery rate-adjusted P-value < 0.05) included *ABCG2*, *ABCC4*, *SLC10A2*, *SLC7A8*, *SLC28A3*, *SLC22A15*, *SLC12A6*, *SLC7A2*, *HNF1A*, *NAT2*, *SLC11A2*, *SLC39A13*, *SLC10A7*, *CYP2E1*, *SLC35F5*, *HNF4A*, *ABCA4*, *SLC19A2* and *SLC17A3* (Figure S1C). Many of these (e.g. *ABCG2*, *ABCC4*, *SLC10A2*, *SLC28A3*, *HNF1A*, *NAT2*, *CYP231*, *HNF4A*) are well-characterized genes involved in drug metabolism and transport, and the transcriptional regulation of ADME genes.

As the cornea and retina contained the highest median levels of gene expression, the biological roles of these genes were further examined (Figure 1B and C). When filtered by expression values, the top 100 genes present in the cornea and retina consisted primarily of SLC transporters (Figure 1B). This is consistent with the greater number of SLC genes included in the custom OpenArray® compared to other genes. The top 100 most highly expressed transporter genes in the cornea and retina were annotated according to their reported functional roles, including xenobiotic and macronutrient transport, with the top fifty genes shown in Figure 1C. Of the top 100 transporter genes located in the cornea and retina, 44% and 50%, respectively, were identified as nutrient and macronutrient transporters. These nutrient transporters were identified as 38% and 46% of the top 50 genes in the cornea and retina, respectively (Figure 1C, red bars). The majority of the macronutrient transporter genes in the subset of most highly expressed genes were carriers for carbohydrates (sugars), amino acids, metal ions and neurotransmitters (Figure 1C). Compared to the retina, the cornea contained a far greater number of drug transporters (29% in the cornea to 13% in the retina) in the 100 most highly expressed genes, and included members of the *SLC22A* organic cation/anion/zwitterion transporter family and several *ABCC* (MRP) efflux transporters. Xenobiotic transporters represented 32% of the top 50 most highly expressed genes in the cornea, and 8% of those in the retina (Figure 1C, blue

bars. In contrast to the cornea, the retina contained a greater proportion of neurotransmitter transporters such as carriers of glutamate and choline, amino acid carriers and ion transporters (Figure 1C, bottom panel, red bars). However, the most highly expressed genes in the retina were associated with transporters that have functions other than nutrient or drug transport, specifically the *SLC25A* family of mitochondrial carriers, which have diverse roles in mitochondrial function and energy metabolism (Figure 1C). In comparison to the retina, the cornea contained a far greater number of drug transporters (29% vs. 13%) in the 100 most highly expressed genes, including many well-characterized members of the *SLC22A* organic cation/anion/zwitterion transporter family, and several of the *ABCC* (MRP) efflux transporters (Figure 1C, blue bars). The expression of numerous drug transporters in the cornea, many of which are known efflux transporters, is consistent with the role of this tissue as a major barrier to ocular drug delivery.

Profiling of drug transporter (Transportal) genes

Transporter genes that may be important for drug transport in the eye were identified by examining TransPortal gene expression levels in all ocular subregions. The top ten most highly expressed TransPortal genes in each ocular tissue are presented in Figure 2. To our knowledge, many of these transporter genes, such as *SLCO1B3*, *ABCC2*, and *ABCC4* in the cornea, have not been previously identified in the various tissues of the human eye (Table 2).

The liver and kidney both have well-characterized drug transport function, and are major sites of drug disposition in the body. Therefore, TransPortal gene expression was compared between the cornea, retina, liver and kidney samples. On average, TransPortal gene expression levels in the cornea were 6.10 fold higher than in the liver and similar to those levels in the kidney (1.36 fold; data not shown). The retina expressed TransPortal genes at levels 4.08 fold higher than the liver, but only at 0.69 fold of the kidney (data not shown). These results indicate that key transporter genes known to influence drug disposition in the liver and kidney are also present at similar, if not higher, transcript levels in the cornea and retina.

To identify TransPortal genes with similar expression patterns in the five eye regions, unsupervised hierarchical cluster analysis was performed (Figure S1C). Twenty-seven TransPortal genes were variably expressed ($SD > 0$) in the eye tissues studied. Several well-defined clusters of differentially expressed genes emerged among the different regions. Notably, a cluster comprised of *ABCB11*, *ABCC2*, *SLC22A3*, *SLC22A6*, *SLC22A7* and *SLC15A1* had uniquely high expression in the cornea versus all other eye regions (Figure S1C). In addition, the retina contained two clusters, each of which contained a single, highly-expressed gene (*ABCC5* and *ABCG2*). Together, these analyses identified several genes that may serve as potential ocular drug targets in the cornea and retina.

IPA was used to investigate the functional relationships among TransPortal gene (listed in Table 2) expression patterns and corneal diseases, in particular herpetic stromal keratitis (HSK), one of the most common causes of blindness in the developed world [37]. Damage to corneal cell layers by recurrent herpetic infection increases corneal opacity resulting in decreased visual acuity. The association of TransPortal genes with HSK was analyzed by

generating and merging networks of the TransPortal genes with IPA-curated pathways for HSK (Figure S2), with the top-scoring ($P=2.32E-14$) network of corneal TransPortal genes selected for further evaluation. Within the HSK network, *SLC22A7* emerged as the most highly expressed gene (log ratio=2.86), whereas *SLCO1A2* was the most weakly expressed gene (log ratio=-3.85) (Figure S2). The merged network revealed complex inter-relationships based upon regulation of gene expression and shared molecular interactions. Within the merged network, two major hubs emerged, consisting of highly interconnected nodes interacting with two central nodes, the inflammatory response gene, *IL1B*, and the transcription factor *HNF4A*, respectively. The analysis suggested that many TransPortal genes are regulated by a variety of immunological mediators and well-characterized post-translational modifiers, such as PXR and CAR, and also serve as important mediators of molecular pathways within the human cornea.

Localization of drug transporters in the cornea and retina

Seven highly expressed TransPortal genes (*ABCC1*, *ABCC2*, *ABCC4*, *ABCC5*, *ABCG2*, *SLC22A3*, *SLC22A7*) were further evaluated by IHC to determine their cellular localization within the cornea. BCRP (*ABCG2*), OCT3 (*SLC22A3*), MRP4 (*ABCC4*) and OAT2 (*SLC22A7*) all localized to the corneal epithelium (Figure 3). OCT3 also was expressed in the corneal endothelium (Figure 3C). In contrast, MRP1 (*ABCC1*), MRP2 (*ABCC2*) and MRP5 (*ABCC5*) were undetectable in the entire cornea (data not shown). Five genes (*ABCC1*, *ABCC5*, *ABCG2*, *SLC22A3*, and *SLCO1B3*) were profiled in the retina by IHC (Figure 4). OCT3 was expressed in the RPE and rod and cones, with the highest expression levels observed in the rods and cones (Figure 4B). BCRP was expressed at higher levels in the outer plexiform and nerve fiber layers than in the inner and outer nuclear layer, and ganglion cells (Figure 4C). Interestingly, BCRP does not appear to be expressed in large ($> 20 \mu\text{m}$) blood vessels of the retina (asterisk in Figure 4C). Furthermore, the positive staining pattern in the retina was confirmed to be BCRP-specific, and not due to non-specific interactions of the primary or secondary antibodies (Supplemental Figure S3). MRP1, MRP5 and OATP1B3 expression were undetectable in all regions of the retina (data not shown).

To date, few studies have examined the expression of drug transporter genes in specific ocular disease states. To compare reported expression and association of the transporters shown in Figure 3 and Figure 4 with ocular disease, we queried the online databases Online Mendelian Inheritance in Man (OMIM) (<http://www.ncbi.nlm.nih.gov/omim>) and the National Eye Institute's NEIBank (<http://neibank.nei.nih.gov/index.shtml>). Our search identified reports of altered expression levels for BCRP and MRP4 in disorders affecting the retina (Supplemental Table S4). In particular, Bcrp and Mrp4 showed reduced expression in a mouse model of oxygen-induced retinopathy (Supplemental Table S4). While no reports of OCT3/Oct3 or OAT2/Oat2 expression in ocular disease states exist, the genes encoding these proteins are predicted to be in linkage disequilibrium with candidate loci for ocular disorders affecting the lens and retina, and may play a role in development or progression of these diseases (Supplemental Table S4).

Validation of SLC22A7 (OAT2) as an ocular drug target

As noted above, *SLC22A7* (OAT2) was identified as a highly-expressed corneal gene also present within a network of genes involved in inflammatory responses to viral infection. We investigated the role of this gene in the transport of acyclovir, a drug used in the treatment of HSK in the cornea [38]. In OAT2-overexpressing HEK293 cells, acyclovir transport was 40 fold higher than empty vector transfected HEK293 cells, and 8 fold higher than PAH, a previously established model substrate for OAT2 (Figure 5A). OAT2-transfected cells transported acyclovir with moderate affinity and high capacity ($K_m=142\pm 50 \mu\text{M}$, $V_{\text{max}}=1721\pm 220 \text{ pmol mg protein}^{-1} \text{ minute}^{-1}$), supporting its role as a selective carrier for acyclovir in the eye (Figure 5B). The selectivity of acyclovir transport by selected OAT family members expressed in the cornea was assessed using HEK293 cells expressing OAT1-4. The functionality of each transporter was determined using each transporter's model substrate (data not shown). Uptake of acyclovir by OAT2 was 21 fold greater than OAT1 and OAT3 (Figure 5C). In contrast, acyclovir was not a substrate for OAT4. Furthermore, OAT2 more efficiently transported acyclovir than OAT1, as indicated by the respective ratios of acyclovir to PAH uptake of 29 and 0.055, consistent with OAT2 being the major transporter for acyclovir.

Discussion

Several transporter genes that may influence ocular drug disposition were identified in ocular tissues through comparative bioinformatic analysis of the mRNA expression profiles of 445 genes. This included genes for transporters, metabolic enzymes, transcription factors and nuclear receptors. Large scale expression profiling of transporter genes detected 97% of the array transcripts in the eye, consistent with the observation that >90% of genes within the human genome are expressed in one or more ocular tissues [39]. Expression profiles of the array genes (the majority of which are for transporters) differed among the five ocular tissues investigated, with the highest expression of array genes in the retina and cornea. Both the retina and cornea manifested high levels of transporter gene expression, particularly for known efflux transporters. Given the endothelial and epithelial cell barriers found in the retina and cornea, their enrichment in transporter transcripts is consistent with their roles in maintaining barrier tissue homeostasis [8, 9]. Reflecting its sensory detection and processing functions, the retina also expressed high levels of genes for neurotransmitter transporters. However, the most highly expressed transporter genes in the retina were from the *SLC25A* family of mitochondrial carriers, consistent with the high rate of oxidative metabolism conducted in the retina [40].

Functional annotation of the most highly expressed transporter genes in the cornea and retina (Figure 1C) indicated that the cornea had the highest expression levels of drug transporter genes, which may serve as important targets for transcorneal delivery of ophthalmics. The highly expressed efflux transporters *ABCC2* and *ABCC5* may serve as a barrier to the absorption of anionic drug substrates such as acyclovir by the cornea. In the retina, *ABCA4* was among the most highly expressed transporters in the retina (Figure 1C). The *ABCA* genes play important roles in the progression of various central nervous system disorders involving cholesterol and lipid accumulation, including age-related macular

degeneration (AMD) [41-43]. Age-related macular degeneration (AMD) is a complex, heterogeneous disorder that is characterized by accumulation of lipid and lipoprotein deposits and formation of lesions in the RPE, leading to progressive or sudden vision loss [44]. Recent genome-wide association studies have implicated *ABCA1* in the development of the most common, chronic subtype of age-related macular degeneration (termed 'dry' AMD) [45, 46], potentially through faulty lipid transport in the RPE. This may contribute to the excessive accumulation of lipid deposits (drusen) in the retina, leading to the degeneration of RPE cells, localized inflammatory responses and neovascularization, with the resulting loss of visual acuity [47]. Even though *ABCA1* was not among the most highly expressed retinal transporter genes, it was expressed in the top 51% of all transporter genes detected in the retina (data not shown). Additional *ABCA* genes having functional overlap with *ABCA1*, such as *ABCA4* [48], may also be associated with dry AMD [42, 43]. Previous genome-wide studies also suggest that, *SLC10A7*, among the top 100 most highly expressed genes in the retina (Figure 1C) is also a candidate gene for the development of dry AMD [45]. Unlike its other family members, the function of *SLC10A7* remains to be investigated, as it does not transport bile acids and steroid sulfates when expressed in *Xenopus laevis* oocytes and HEK293 cells [49].

Profiling of genes of relevance to drug disposition (e.g., the TransPortal genes) in ocular tissues indicated that the expression patterns of corneal TransPortal genes is correlated with inflammatory regulators *IL1B* and *HNF4A* (Figure S2). The critical pro-inflammatory cytokine *IL1 β* is produced in the corneal epithelium and is involved in apoptosis, tissue repair, proliferation and differentiation (for a review, see Bensi, et al. [50]). *HNF4A* represents a major network hub with significantly enriched expression in the eye ($\log_{FC}=2.73$, $P=0.0013$; Table S3) and as a nuclear transcription factor regulates the expression of the TransPortal genes *SLC22A7*, *ABCB11*, *ABCC2*, *ABCC6*, *SLC22A1*, *ABCA1*, and *ABCB1*, and possibly *SLC22A3*, *ABCC3* and *SLC10A1* [51-53]. Given the involvement of *IL1B* [54] and *HNF4A* [55, 56] in chronic, autoinflammatory states [55, 56], this sub-network of genes likely serve important roles in corneal surface inflammatory diseases, warranting further characterization [57-59].

Through mRNA and protein expression profiling, network pathway modeling and prioritization of pharmacologically-relevant genes, *SLC22A7* (OAT2) was identified as a key network node for HSK in the cornea. OAT2 transports cyclic guanosine monophosphate (cGMP) [36], an important second messenger in mammalian phototransduction [60]. In addition, OAT2 transports acyclovir, a widely prescribed treatment for HSK [61]. OAT2 was localized in the corneal epithelial layer, where it may transport acyclovir and other substrates through the corneal matrix into the anterior chamber (Figure 3). The role of OAT2 in corneal acyclovir transport has important implications for the treatment of herpes simplex virus (HSV) infections, providing a co-development target for topically administered anti-herpetics. In addition to the role of OAT2 in acyclovir transport, inhibitors of BCRP enhance acyclovir accumulation *in vitro*, suggesting a role for BCRP in transcorneal acyclovir transport [58]. BCRP mRNA and protein are also expressed in corneal epithelium (Figures 3 and 4), and *ABCG2* was identified as a network node regulated by *IL1B* in the cornea (Figure S2). Corneal damage in HSK also activates expression of *IL1B* and *HNF4A*,

altering the expression of genes they regulate [59]. Together, these data suggest that *SLC22A7* and *ABCG2* are involved in transcorneal transport of acyclovir and the severity of the inflammatory response to that infection.

In addition to its corneal expression, BCRP was highly expressed in the retina, with its primary localization in the nerve fiber layers (Figure 4C). While BCRP is reportedly expressed in the blood vessels forming the mouse inner blood-retinal barrier (BRB) and in the conditionally immortalized rat retinal capillary endothelial cell line, TR-iBRB [62] (Table 2), it was not detected in large (> 20 μm) blood vessels of the nerve fiber layer (Figure 4C). Since BCRP primarily effluxes intracellular substrates into the extracellular space, this expression pattern suggests that BCRP may act to protect retinal nerve fibers from injury by removing intracellular toxins and xenobiotics. For example, a recent study investigating the mechanism of retinal degeneration and blindness in cats due to fluorquinolone exposure found that feline BCRP is functionally defective and fails to provide adequate protection against enrofloxacin-induced phototoxicity [61].

In glaucoma, loss of the retinal ganglion cells and their optic nerve axons leads to elevation of intraocular pressure. Brimonidine, a non-selective α_2 -adrenergic receptor agonist which is prescribed for treatment of open-angle glaucoma or ocular hypertension, was also recently shown to be neuroprotective in the retina [63]. Due to its ability to lower intraocular pressure and also preserve axonal transport, brimonidine may directly inhibit the progression of glaucoma. A cationic drug, brimonidine requires a carrier-mediated uptake mechanism in order to permeate cell membranes. Brimonidine has been shown to accumulate in bovine RPE and ARPE-19 cell monolayers by a carrier-mediated process that is sensitive to some organic cation transporter inhibitors [64]. Due to their substrate specificity for organic cations, the *SLC22A* family members represent likely carriers for brimonidine; however, the exact transport mechanism has not yet been identified. We found that the organic cation transporter OCT3 was expressed in the RPE (Figure 4B), consistent with previous observations of OCT3 mRNA expression in mouse retina and the human RPE cell line, ARPE-19 [65] (Table 2). OCT3 may therefore enhance organic cation penetration into the retina, particularly through the RPE.

In summary, the transcript levels of 445 transporters, drug metabolizing enzymes, transcription factors and nuclear receptors were profiled in an effort to identify potential therapeutic drug targets within the eye. Through RNA expression profiling, immunohistochemistry and bioinformatic analyses, we have identified several transporters that may potentially play a role in drug disposition within the regions of the eye, including OAT2 in the cornea and BCRP and OCT3 in the retina. These findings have implications for guiding drug design strategies to achieve tissue-specific drug delivery in the eye through selective targeting of ocular transporters.

Supplementary Material

Refer to Web version on PubMed Central for supplementary material.

Acknowledgments

The authors thank Ms. Jeannie Powers for her administrative support. The authors are grateful for the financial support of this work by Allergan, Inc. (support for A.B., D.T., E.G. and S.S.) and National Institute of Health grants U19GM061390 (support for C.C. and K.G.). A.D. acknowledges financial support from National Institute of Health Fellowship R25 CA112355 (support for A.D.).

References

1. Qazi Y, Wong G, Monson B, Stringham J, Ambati BK. Corneal transparency: genesis, maintenance and dysfunction. *Brain Res Bull.* 2010; 81:198–210. [PubMed: 19481138]
2. Pitkanen L, Ranta VP, Moilanen H, Urtti A. Permeability of retinal pigment epithelium: effects of permeant molecular weight and lipophilicity. *Invest Ophthalmol Vis Sci.* 2005; 46:641–646. [PubMed: 15671294]
3. Ranta VP, Mannermaa E, Lummeppo K, Subrizi A, Laukkanen A, Antopolsky M, Murtomaki L, Hornof M, Urtti A. Barrier analysis of periocular drug delivery to the posterior segment. *J Control Release.* 2010; 148:42–48. [PubMed: 20831888]
4. Prausnitz MR, Noonan JS. Permeability of cornea, sclera, and conjunctiva: a literature analysis for drug delivery to the eye. *J Pharm Sci.* 1998; 87:1479–1488. [PubMed: 10189253]
5. Lawrence MS, Miller JW. Ocular tissue permeabilities. *Int Ophthalmol Clin.* 2004; 44:53–61. [PubMed: 15211177]
6. Hamalainen KM, Kananen K, Auriola S, Kontturi K, Urtti A. Characterization of paracellular and aqueous penetration routes in cornea, conjunctiva, and sclera. *Invest Ophthalmol Vis Sci.* 1997; 38:627–634. [PubMed: 9071216]
7. Tomi M, Hosoya K. The role of blood-ocular barrier transporters in retinal drug disposition: an overview. *Expert Opin Drug Metab Toxicol.* 2010; 6:1111–1124. [PubMed: 20438316]
8. Hediger MA, Romero MF, Peng JB, Rolfs A, Takanaga H, Bruford EA. The ABCs of solute carriers: physiological, pathological and therapeutic implications of human membrane transport proteins. *Introduction. Pflugers Arch.* 2004; 447:465–468. [PubMed: 14624363]
9. Holland IB. ABC transporters, mechanisms and biology: an overview. *Essays Biochem.* 2011; 50:1–17. [PubMed: 21967049]
10. Borst P, Elferink RO. Mammalian ABC transporters in health and disease. *Annu Rev Biochem.* 2002; 71:537–592. [PubMed: 12045106]
11. Hagenbuch B. Molecular properties of hepatic uptake systems for bile acids and organic anions. *J Membr Biol.* 1997; 160:1–8. [PubMed: 9351887]
12. Hagenbuch B, Gao B, Meier PJ. Transport of xenobiotics across the blood-brain barrier. *News Physiol Sci.* 2002; 17:231–234. [PubMed: 12433976]
13. Hagenbuch B. Drug uptake systems in liver and kidney: a historic perspective. *Clin Pharmacol Ther.* 2010; 87:39–47. [PubMed: 19924123]
14. Koepsell H. Organic cation transporters in intestine, kidney, liver, and brain. *Annu Rev Physiol.* 1998; 60:243–266. [PubMed: 9558463]
15. Nigam SK, Bush KT, Bhatnagar V. Drug and toxicant handling by the OAT organic anion transporters in the kidney and other tissues. *Nat Clin Pract Nephrol.* 2007; 3:443–448. [PubMed: 17653123]
16. Schinkel AH, Jonker JW. Mammalian drug efflux transporters of the ATP binding cassette (ABC) family: an overview. *Adv Drug Deliv Rev.* 2003; 55:3–29. [PubMed: 12535572]
17. Sweet DH, Bush KT, Nigam SK. The organic anion transporter family: from physiology to ontogeny and the clinic. *Am J Physiol Renal Physiol.* 2001; 281:F197–205. [PubMed: 11457711]
18. You G. The role of organic ion transporters in drug disposition: an update. *Curr Drug Metab.* 2004; 5:55–62. [PubMed: 14965250]
19. Mahringer A, Ott M, Reimold I, Reichel V, Fricker G. The ABC of the blood-brain barrier - regulation of drug efflux pumps. *Curr Pharm Des.* 2011; 17:2762–2770. [PubMed: 21827407]
20. Pardridge WM. Advances in cell biology of blood-brain barrier transport. *Semin Cell Biol.* 1991; 2:419–426. [PubMed: 1813031]

21. Dahlin A, Royall J, Hohmann JG, Wang J. Expression profiling of the solute carrier gene family in the mouse brain. *J Pharmacol Exp Ther*. 2009; 329:558–570. [PubMed: 19179540]
22. Dahlin A, Xia L, Kong W, Hevner R, Wang J. Expression and immunolocalization of the plasma membrane monoamine transporter in the brain. *Neuroscience*. 2007; 146:1193–1211. [PubMed: 17408864]
23. Robillard KR, Hoque T, Bendayan R. Expression of ATP-binding cassette membrane transporters in rodent and human sertoli cells: relevance to the permeability of antiretroviral therapy at the blood-testis barrier. *J Pharmacol Exp Ther*. 2012; 340:96–108. [PubMed: 21990609]
24. Pelletier RM. The blood-testis barrier: the junctional permeability, the proteins and the lipids. *Prog Histochem Cytochem*. 2011; 46:49–127. [PubMed: 21705043]
25. Huls M, Russel FG, Masereeuw R. The role of ATP binding cassette transporters in tissue defense and organ regeneration. *J Pharmacol Exp Ther*. 2009; 328:3–9. [PubMed: 18791064]
26. Mannermaa E, Vellonen KS, Urtti A. Drug transport in corneal epithelium and blood-retina barrier: emerging role of transporters in ocular pharmacokinetics. *Adv Drug Deliv Rev*. 2006; 58:1136–1163. [PubMed: 17081648]
27. Hosoya K, Makihara A, Tsujikawa Y, Yoneyama D, Mori S, Terasaki T, Akanuma S, Tomi M, Tachikawa M. Roles of inner blood-retinal barrier organic anion transporter 3 in the vitreous/retina-to-blood efflux transport of p-aminohippuric acid, benzylpenicillin, and 6-mercaptopurine. *J Pharmacol Exp Ther*. 2009; 329:87–93. [PubMed: 19116370]
28. Hosoya K, Tomi M. Advances in the cell biology of transport via the inner blood-retinal barrier: establishment of cell lines and transport functions. *Biol Pharm Bull*. 2005; 28:1–8. [PubMed: 15635153]
29. Tagami M, Kusuhara S, Honda S, Tsukahara Y, Negi A. Expression of ATP-binding cassette transporters at the inner blood-retinal barrier in a neonatal mouse model of oxygen-induced retinopathy. *Brain Res*. 2009; 1283:186–193. [PubMed: 19505448]
30. Zhang T, Xiang CD, Gale D, Carreiro S, Wu EY, Zhang EY. Drug transporter and cytochrome P450 mRNA expression in human ocular barriers: implications for ocular drug disposition. *Drug Metab Dispos*. 2008; 36:1300–1307. [PubMed: 18411399]
31. Juuti-Uusitalo K, Vaajasaari H, Ryhanen T, Narkilahti S, Suuronen R, Mannermaa E, Kaarniranta K, Skottman H. Efflux protein expression in human stem cell-derived retinal pigment epithelial cells. *PLoS One*. 2012; 7:e30089. [PubMed: 22272278]
32. Giacomini KM, Huang SM, Tweedie DJ, Benet LZ, Brouwer KL, Chu X, Dahlin A, Evers R, Fischer V, Hillgren KM, Hoffmaster KA, Ishikawa T, Keppler D, Kim RB, Lee CA, Niemi M, Polli JW, Sugiyama Y, Swaan PW, Ware JA, Wright SH, Yee SW, Zamek-Gliszczynski MJ, Zhang L. Membrane transporters in drug development. *Nat Rev Drug Discov*. 2010; 9:215–236. [PubMed: 20190787]
33. Pfaffl MW. A new mathematical model for relative quantification in real-time RT-PCR. *Nucleic Acids Res*. 2001; 29:e45. [PubMed: 11328886]
34. Team, RDC. R Foundation for Statistical Computing. Vienna, Austria: 2011. R: A language and environment for *statistical computing*.
35. Culhane AC, Thioulouse J, Perriere G, Higgins DG. MADE4: an R package for multivariate analysis of gene expression data. *Bioinformatics*. 2005; 21:2789–2790. [PubMed: 15797915]
36. Cropp CD, Komori T, Shima JE, Urban TJ, Yee SW, More SS, Giacomini KM. Organic anion transporter 2 (SLC22A7) is a facilitative transporter of cGMP. *Mol Pharmacol*. 2008; 73:1151–1158. [PubMed: 18216183]
37. Farooq AV, Shukla D. Herpes Simplex Epithelial and Stromal Keratitis: An Epidemiologic Update. *Surv Ophthalmol*. 2012
38. Acyclovir for the prevention of recurrent herpes simplex virus eye disease. Herpetic Eye Disease Study Group. *N Engl J Med*. 1998; 339:300–306. [PubMed: 9696640]
39. Sheffield VC, Stone EM. Genomics and the eye. *N Engl J Med*. 2011; 364:1932–1942. [PubMed: 21591945]
40. Yu DY, Cringle SJ. Oxygen distribution and consumption within the retina in vascularised and avascular retinas and in animal models of retinal disease. *Prog Retin Eye Res*. 2001; 20:175–208. [PubMed: 11173251]

41. Zarepari S, Buraczynska M, Branham KE, Shah S, Eng D, Li M, Pawar H, Yashar BM, Moroi SE, Lichter PR, Petty HR, Richards JE, Abecasis GR, Elner VM, Swaroop A. Toll-like receptor 4 variant D299G is associated with susceptibility to age-related macular degeneration. *Hum Mol Genet.* 2005; 14:1449–1455. [PubMed: 15829498]
42. Fritsche LG, Fleckenstein M, Fiebig BS, Schmitz-Valckenberg S, Bindewald-Wittich A, Keilhauer CN, Renner AB, Mackensen F, Mossner A, Pauleikhoff D, Adrion C, Mansmann U, Scholl HP, Holz FG, Weber BH. A subgroup of age-related macular degeneration is associated with mono-allelic sequence variants in the ABCA4 gene. *Invest Ophthalmol Vis Sci.* 2012; 53:2112–2118. [PubMed: 22427542]
43. Queller G, Russell SR, Scheetz TE, Stone EM, Abramoff MD. Computational quantification of complex fundus phenotypes in age-related macular degeneration and Stargardt disease. *Invest Ophthalmol Vis Sci.* 2011; 52:2976–2981. [PubMed: 21310908]
44. Ebrahimi KB, Handa JT. Lipids, lipoproteins, and age-related macular degeneration. *J Lipids.* 2011; 2011:802059. [PubMed: 21822496]
45. Chen W, Stambolian D, Edwards AO, Branham KE, Othman M, Jakobsdottir J, Tosakulwong N, Pericak-Vance MA, Campochiaro PA, Klein ML, Tan PL, Conley YP, Kanda A, Kopplin L, Li Y, Augustaitis KJ, Karoukis AJ, Scott WK, Agarwal A, Kovach JL, Schwartz SG, Postel EA, Brooks M, Baratz KH, Brown WL, Brucker AJ, Orlin A, Brown G, Ho A, Regillo C, Donoso L, Tian L, Kaderli B, Hadley D, Hagstrom SA, Peachey NS, Klein R, Klein BE, Gotoh N, Yamashiro K, Ferris Iii F, Fagerness JA, Reynolds R, Farrer LA, Kim IK, Miller JW, Corton M, Carracedo A, Sanchez-Salorio M, Pugh EW, Doheny KF, Brion M, Deangelis MM, Weeks DE, Zack DJ, Chew EY, Heckenlively JR, Yoshimura N, Iyengar SK, Francis PJ, Katsanis N, Seddon JM, Haines JL, Gorin MB, Abecasis GR, Swaroop A. Genetic variants near TIMP3 and high-density lipoprotein-associated loci influence susceptibility to age-related macular degeneration. *Proc Natl Acad Sci U S A.* 2010; 107:7401–7406. [PubMed: 20385819]
46. Yu Y, Reynolds R, Fagerness J, Rosner B, Daly MJ, Seddon JM. Association of variants in the LIPC and ABCA1 genes with intermediate and large drusen and advanced age-related macular degeneration. *Invest Ophthalmol Vis Sci.* 2011; 52:4663–4670. [PubMed: 21447678]
47. Duncan KG, Hosseini K, Bailey KR, Yang H, Lowe RJ, Matthes MT, Kane JP, LaVail MM, Schwartz DM, Duncan JL. Expression of reverse cholesterol transport proteins ATP-binding cassette A1 (ABCA1) and scavenger receptor BI (SR-BI) in the retina and retinal pigment epithelium. *Br J Ophthalmol.* 2009; 93:1116–1120. [PubMed: 19304587]
48. Kaminski WE, Piehler A, Wenzel JJ. ABC A-subfamily transporters: structure, function and disease. *Biochim Biophys Acta.* 2006; 1762:510–524. [PubMed: 16540294]
49. Godoy JR, Fernandes C, Doring B, Beuerlein K, Petzinger E, Geyer J. Molecular and phylogenetic characterization of a novel putative membrane transporter (SLC10A7), conserved in vertebrates and bacteria. *Eur J Cell Biol.* 2007; 86:445–460. [PubMed: 17628207]
50. Bensi G, Raugei G, Palla E, Carinci V, Tornese Buonamassa D, Melli M. Human interleukin-1 beta gene. *Gene.* 1987; 52:95–101. [PubMed: 2954882]
51. Popowski K, Eloranta JJ, Saborowski M, Fried M, Meier PJ, Kullak-Ublick GA. The human organic anion transporter 2 gene is transactivated by hepatocyte nuclear factor-4 alpha and suppressed by bile acids. *Mol Pharmacol.* 2005; 67:1629–1638. [PubMed: 15692145]
52. Kamiyama Y, Matsubara T, Yoshinari K, Nagata K, Kamimura H, Yamazoe Y. Role of human hepatocyte nuclear factor 4alpha in the expression of drug-metabolizing enzymes and transporters in human hepatocytes assessed by use of small interfering RNA. *Drug Metab Pharmacokin.* 2007; 22:287–298. [PubMed: 17827783]
53. Douet V, VanWart CM, Heller MB, Reinhard S, Le Saux O. HNF4alpha and NF-E2 are key transcriptional regulators of the murine Abcc6 gene expression. *Biochim Biophys Acta.* 2006; 1759:426–436. [PubMed: 16997394]
54. Dinarello CA. Blocking interleukin-1beta in acute and chronic autoinflammatory diseases. *J Intern Med.* 2011; 269:16–28. [PubMed: 21158974]
55. Barrett JC, Lee JC, Lees CW, Prescott NJ, Anderson CA, Phillips A, Wesley E, Parnell K, Zhang H, Drummond H, Nimmo ER, Massey D, Blaszczyk K, Elliott T, Cotterill L, Dallal H, Lobo AJ, Mowat C, Sanderson JD, Jewell DP, Newman WG, Edwards C, Ahmad T, Mansfield JC, Satsangi J, Parkes M, Mathew CG, Donnelly P, Peltonen L, Blackwell JM, Bramon E, Brown MA, Casas

- JP, Corvin A, Craddock N, Deloukas P, Duncanson A, Jankowski J, Markus HS, McCarthy MI, Palmer CN, Plomin R, Rautanen A, Sawcer SJ, Samani N, Trembath RC, Viswanathan AC, Wood N, Spencer CC, Bellenguez C, Davison D, Freeman C, Strange A, Langford C, Hunt SE, Edkins S, Gwilliam R, Blackburn H, Bumpstead SJ, Dronov S, Gillman M, Gray E, Hammond N, Jayakumar A, McCann OT, Liddle J, Perez ML, Potter SC, Ravindrarajah R, Rickets M, Waller M, Weston P, Widaa S, Whittaker P, Attwood AP, Stephens J, Sambrook J, Ouwehand WH, McArdle WL, Ring SM, Strachan DP. Genome-wide association study of ulcerative colitis identifies three new susceptibility loci, including the HNF4A region. *Nat Genet.* 2009; 41:1330–1334. [PubMed: 19915572]
56. Dehghan A, Dupuis J, Barbalic M, Bis JC, Eiriksdottir G, Lu C, Pellikka N, Wallaschofski H, Kettunen J, Henneman P, Baumert J, Strachan DP, Fuchsberger C, Vitart V, Wilson JF, Pare G, Naitza S, Rudock ME, Surakka I, de Geus EJ, Alizadeh BZ, Guralnik J, Shuldiner A, Tanaka T, Zee RY, Schnabel RB, Nambi V, Kavousi M, Ripatti S, Nauck M, Smith NL, Smith AV, Sundvall J, Scheet P, Liu Y, Ruukonen A, Rose LM, Larson MG, Hoogeveen RC, Freimer NB, Teumer A, Tracy RP, Launer LJ, Buring JE, Yamamoto JF, Folsom AR, Sijbrands EJ, Pankow J, Elliott P, Keane JF, Sun W, Sarin AP, Fontes JD, Badola S, Astor BC, Hofman A, Pouta A, Werdan K, Greiser KH, Kuss O, Meyer zu Schwabedissen HE, Thiery J, Jamshidi Y, Nolte IM, Soranzo N, Spector TD, Volzke H, Parker AN, Aspelund T, Bates D, Young L, Tsui K, Siscovick DS, Guo X, Rotter JJ, Uda M, Schlessinger D, Rudan I, Hicks AA, Penninx BW, Thorand B, Gieger C, Coresh J, Willemsen G, Harris TB, Uitterlinden AG, Jarvelin MR, Rice K, Radke D, Salomaa V, Willems van Dijk K, Boerwinkle E, Vasani RS, Ferrucci L, Gibson QD, Bandinelli S, Snieder H, Boomsma DI, Xiao X, Campbell H, Hayward C, Pramstaller PP, van Duijn CM, Peltonen L, Psaty BM, Gudnason V, Ridker PM, Homuth G, Koenig W, Ballantyne CM, Witteman JC, Benjamin EJ, Perola M, Chasman DI. Meta-analysis of genome-wide association studies in >80 000 subjects identifies multiple loci for C-reactive protein levels. *Circulation.* 2011; 123:731–738. [PubMed: 21300955]
57. Cheng Y, Vapurcuyan A, Shahidullah M, Aleksunes LM, Pelis RM. Expression of organic anion transporter 2 in the human kidney and its potential role in the tubular secretion of guanine-containing antiviral drugs. *Drug Metab Dispos.* 2012; 40:617–624. [PubMed: 22190696]
58. Gunness P, Aleksa K, Koren G. Acyclovir is a substrate for the human breast cancer resistance protein (BCRP/ABCG2): implications for renal tubular transport and acyclovir-induced nephrotoxicity. *Can J Physiol Pharmacol.* 2011; 89:675–680. [PubMed: 21859328]
59. Streilein JW, Dana MR, Ksander BR. Immunity causing blindness: five different paths to herpes stromal keratitis. *Immunol Today.* 1997; 18:443–449. [PubMed: 9293161]
60. Korenbrot JJ. Speed, adaptation, and stability of the response to light in cone photoreceptors: the functional role of Ca-dependent modulation of ligand sensitivity in cGMP-gated ion channels. *J Gen Physiol.* 2012; 139:31–56. [PubMed: 22200947]
61. Ramirez CJ, Minch JD, Gay JM, Lahmers SM, Guerra DJ, Halderson GJ, Schneider T, Mealey KL. Molecular genetic basis for fluoroquinolone-induced retinal degeneration in cats. *Pharmacogenet Genomics.* 2011; 21:66–75. [PubMed: 21150813]
62. Asashima T, Hori S, Ohtsuki S, Tachikawa M, Watanabe M, Mukai C, Kitagaki S, Miyakoshi N, Terasaki T. ATP-binding cassette transporter G2 mediates the efflux of phototoxins on the luminal membrane of retinal capillary endothelial cells. *Pharm Res.* 2006; 23:1235–1242. [PubMed: 16715370]
63. Lambert WS, Ruiz L, Crish SD, Wheeler LA, Calkins DJ. Brimonidine prevents axonal and somatic degeneration of retinal ganglion cell neurons. *Mol Neurodegener.* 2011; 6:4. [PubMed: 21232114]
64. Zhang N, Kannan R, Okamoto CT, Ryan SJ, Lee VH, Hinton DR. Characterization of brimonidine transport in retinal pigment epithelium. *Invest Ophthalmol Vis Sci.* 2006; 47:287–294. [PubMed: 16384975]
65. Rajan PD, Kekuda R, Chancy CD, Huang W, Ganapathy V, Smith SB. Expression of the extraneuronal monoamine transporter in RPE and neural retina. *Curr Eye Res.* 2000; 20:195–204. [PubMed: 10694895]

66. Li M, Anderson GD, Phillips BR, Kong W, Shen DD, Wang J. Interactions of amoxicillin and cefaclor with human renal organic anion and peptide transporters. *Drug Metab Dispos.* 2006; 34:547–555. [PubMed: 16434549]
67. Guo A, Hu P, Balimane PV, Leibach FH, Sinko PJ. Interactions of a nonpeptidic drug, valacyclovir, with the human intestinal peptide transporter (hPEPT1) expressed in a mammalian cell line. *J Pharmacol Exp Ther.* 1999; 289:448–454. [PubMed: 10087037]
68. Balimane PV, Tamai I, Guo A, Nakanishi T, Kitada H, Leibach FH, Tsuji A, Sinko PJ. Direct evidence for peptide transporter (PepT1)-mediated uptake of a nonpeptide prodrug, valacyclovir. *Biochem Biophys Res Commun.* 1998; 250:246–251. [PubMed: 9753615]
69. Muller J, Lips KS, Metzner L, Neubert RH, Koepsell H, Brandsch M. Drug specificity and intestinal membrane localization of human organic cation transporters (OCT). *Biochem Pharmacol.* 2005; 70:1851–1860. [PubMed: 16263091]
70. Takeda M, Khamdang S, Narikawa S, Kimura H, Kobayashi Y, Yamamoto T, Cha SH, Sekine T, Endou H. Human organic anion transporters and human organic cation transporters mediate renal antiviral transport. *J Pharmacol Exp Ther.* 2002; 300:918–924. [PubMed: 11861798]
71. Kimura H, Takeda M, Narikawa S, Enomoto A, Ichida K, Endou H. Human organic anion transporters and human organic cation transporters mediate renal transport of prostaglandins. *J Pharmacol Exp Ther.* 2002; 301:293–298. [PubMed: 11907186]
72. Amphoux A, Vialou V, Drescher E, Bruss M, Mannoury La Cour C, Rochat C, Millan MJ, Giros B, Bonisch H, Gautron S. Differential pharmacological in vitro properties of organic cation transporters and regional distribution in rat brain. *Neuropharmacology.* 2006; 50:941–952. [PubMed: 16581093]
73. Han YH, Sweet DH, Hu DN, Pritchard JB. Characterization of a novel cationic drug transporter in human retinal pigment epithelial cells. *J Pharmacol Exp Ther.* 2001; 296:450–457. [PubMed: 11160630]
74. Yabuuchi H, Tamai I, Nezu J, Sakamoto K, Oku A, Shimane M, Sai Y, Tsuji A. Novel membrane transporter OCTN1 mediates multispecific, bidirectional, and pH-dependent transport of organic cations. *J Pharmacol Exp Ther.* 1999; 289:768–773. [PubMed: 10215651]
75. Ohashi R, Tamai I, Yabuuchi H, Nezu JI, Oku A, Sai Y, Shimane M, Tsuji A. Na(+)-dependent carnitine transport by organic cation transporter (OCTN2): its pharmacological and toxicological relevance. *J Pharmacol Exp Ther.* 1999; 291:778–784. [PubMed: 10525100]
76. Khamdang S, Takeda M, Babu E, Noshiro R, Onozato ML, Tojo A, Enomoto A, Huang XL, Narikawa S, Anzai N, Piyachaturawat P, Endou H. Interaction of human and rat organic anion transporter 2 with various cephalosporin antibiotics. *Eur J Pharmacol.* 2003; 465:1–7. [PubMed: 12650826]
77. Chu XY, Bleasby K, Yabut J, Cai X, Chan GH, Hafey MJ, Xu S, Bergman AJ, Braun MP, Dean DC, Evers R. Transport of the dipeptidyl peptidase-4 inhibitor sitagliptin by human organic anion transporter 3, organic anion transporting polypeptide 4C1, and multidrug resistance P-glycoprotein. *J Pharmacol Exp Ther.* 2007; 321:673–683. [PubMed: 17314201]
78. Ho ES, Lin DC, Mendel DB, Cihlar T. Cytotoxicity of antiviral nucleotides adefovir and cidofovir is induced by the expression of human renal organic anion transporter 1. *J Am Soc Nephrol.* 2000; 11:383–393. [PubMed: 10703662]
79. Cihlar T, Lin DC, Pritchard JB, Fuller MD, Mendel DB, Sweet DH. The antiviral nucleotide analogs cidofovir and adefovir are novel substrates for human and rat renal organic anion transporter 1. *Mol Pharmacol.* 1999; 56:570–580. [PubMed: 10462545]
80. Cihlar T, Ho ES. Fluorescence-based assay for the interaction of small molecules with the human renal organic anion transporter 1. *Anal Biochem.* 2000; 283:49–55. [PubMed: 10929807]
81. Babu E, Takeda M, Narikawa S, Kobayashi Y, Yamamoto T, Cha SH, Sekine T, Sakthisekaran D, Endou H. Human organic anion transporters mediate the transport of tetracycline. *Jpn J Pharmacol.* 2002; 88:69–76. [PubMed: 11855680]
82. Kobayashi Y, Sakai R, Ohshiro N, Ohbayashi M, Kohyama N, Yamamoto T. Possible involvement of organic anion transporter 2 on the interaction of theophylline with erythromycin in the human liver. *Drug Metab Dispos.* 2005; 33:619–622. [PubMed: 15708966]

83. Kobayashi Y, Ohshiro N, Sakai R, Ohbayashi M, Kohyama N, Yamamoto T. Transport mechanism and substrate specificity of human organic anion transporter 2 (hOat2 [SLC22A7]). *J Pharm Pharmacol.* 2005; 57:573–578. [PubMed: 15901346]
84. Tanihara Y, Masuda S, Sato T, Katsura T, Ogawa O, Inui K. Substrate specificity of MATE1 and MATE2-K, human multidrug and toxin extrusions/H(+)-organic cation antiporters. *Biochem Pharmacol.* 2007; 74:359–371. [PubMed: 17509534]
85. Maeda T, Takahashi K, Ohtsu N, Oguma T, Ohnishi T, Atsumi R, Tamai I. Identification of influx transporter for the quinolone antibacterial agent levofloxacin. *Mol Pharm.* 2007; 4:85–94. [PubMed: 17274666]
86. Gao B, Huber RD, Wenzel A, Vavricka SR, Ismail MG, Reme C, Meier PJ. Localization of organic anion transporting polypeptides in the rat and human ciliary body epithelium. *Exp Eye Res.* 2005; 80:61–72. [PubMed: 15652527]
87. Okabe M, Szakacs G, Reimers MA, Suzuki T, Hall MD, Abe T, Weinstein JN, Gottesman MM. Profiling SLCO and SLC22 genes in the NCI-60 cancer cell lines to identify drug uptake transporters. *Mol Cancer Ther.* 2008; 7:3081–3091. [PubMed: 18790787]
88. Kraft ME, Glaeser H, Mandery K, Konig J, Auge D, Fromm MF, Schlotzer-Schrehardt U, Welge-Lussen U, Kruse FE, Zolk O. The prostaglandin transporter OATP2A1 is expressed in human ocular tissues and transports the antiglaucoma prostanoid latanoprost. *Invest Ophthalmol Vis Sci.* 2010; 51:2504–2511. [PubMed: 20019365]
89. Mannermaa E, Vellonen KS, Ryhanen T, Kokkonen K, Ranta VP, Kaarniranta K, Urtti A. Efflux protein expression in human retinal pigment epithelium cell lines. *Pharm Res.* 2009; 26:1785–1791. [PubMed: 19384462]
90. Vellonen KS, Mannermaa E, Turner H, Hakli M, Wolosin JM, Tervo T, Honkakoski P, Urtti A. Effluxing ABC transporters in human corneal epithelium. *J Pharm Sci.* 2010; 99:1087–1098. [PubMed: 19623615]
91. Kawazu K, Yamada K, Nakamura M, Ota A. Characterization of cyclosporin A transport in cultured rabbit corneal epithelial cells: P-glycoprotein transport activity and binding to cyclophilin. *Invest Ophthalmol Vis Sci.* 1999; 40:1738–1744. [PubMed: 10393043]
92. Kawazu K, Oshita A, Nakamura T, Nakashima M, Ichikawa N, Sasaki H. Transport of acebutolol through rabbit corneal epithelium. *Biol Pharm Bull.* 2006; 29:846–849. [PubMed: 16595934]
93. Hariharan S, Gunda S, Mishra GP, Pal D, Mitra AK. Enhanced corneal absorption of erythromycin by modulating P-glycoprotein and MRP mediated efflux with corticosteroids. *Pharm Res.* 2009; 26:1270–1282. [PubMed: 18958406]
94. Kimura Y, Kioka N, Kato H, Matsuo M, Ueda K. Modulation of drug-stimulated ATPase activity of human MDR1/P-glycoprotein by cholesterol. *Biochem J.* 2007; 401:597–605. [PubMed: 17029589]
95. Karssen AM, Meijer OC, van der Sandt IC, De Boer AG, De Lange EC, De Kloet ER. The role of the efflux transporter P-glycoprotein in brain penetration of prednisolone. *J Endocrinol.* 2002; 175:251–260. [PubMed: 12379510]
96. Smith AJ, van Helvoort A, van Meer G, Szabo K, Welker E, Szakacs G, Varadi A, Sarkadi B, Borst P. MDR3 P-glycoprotein, a phosphatidylcholine translocase, transports several cytotoxic drugs and directly interacts with drugs as judged by interference with nucleotide trapping. *J Biol Chem.* 2000; 275:23530–23539. [PubMed: 10918072]
97. Karla PK, Pal D, Quinn T, Mitra AK. Molecular evidence and functional expression of a novel drug efflux pump (ABCC2) in human corneal epithelium and rabbit cornea and its role in ocular drug efflux. *Int J Pharm.* 2007; 336:12–21. [PubMed: 17156953]
98. Karla PK, Quinn TL, Herndon BL, Thomas P, Pal D, Mitra A. Expression of multidrug resistance associated protein 5 (MRP5) on cornea and its role in drug efflux. *J Ocul Pharmacol Ther.* 2009; 25:121–132. [PubMed: 19323627]
99. Stojic J, Stohr H, Weber BH. Three novel ABCC5 splice variants in human retina and their role as regulators of ABCC5 gene expression. *BMC Mol Biol.* 2007; 8:42. [PubMed: 17521428]
100. Karla PK, Earla R, Boddu SH, Johnston TP, Pal D, Mitra A. Molecular expression and functional evidence of a drug efflux pump (BCRP) in human corneal epithelial cells. *Curr Eye Res.* 2009; 34:1–9. [PubMed: 19172464]

101. Wilson MW, Fraga CH, Fuller CE, Rodriguez-Galindo C, Mancini J, Hagedorn N, Leggas ML, Stewart CF. Immunohistochemical detection of multidrug-resistant protein expression in retinoblastoma treated by primary enucleation. *Invest Ophthalmol Vis Sci.* 2006; 47:1269–73. [PubMed: 16565357]
102. Tagami M, Kusuhara S, Imai H, Uemura A, Honda S, Tsukahara Y, Negi A. MRP4 knockdown enhances migration, suppresses apoptosis, and produces aggregated morphology in human retinal vascular endothelial cells. *Biochem Biophys Res Commun.* 2010; 400:593–8. [PubMed: 20804728]
103. Wistow G, Peterson K, Gao J, Buchoff P, Jaworski C, Bowes-Rickman C, Ebright JN, Hauser MA, Hoover D. NEIBank: genomics and bioinformatics resources for vision research. *Mol Vis.* 2008; 14:1327–37. [PubMed: 18648525]

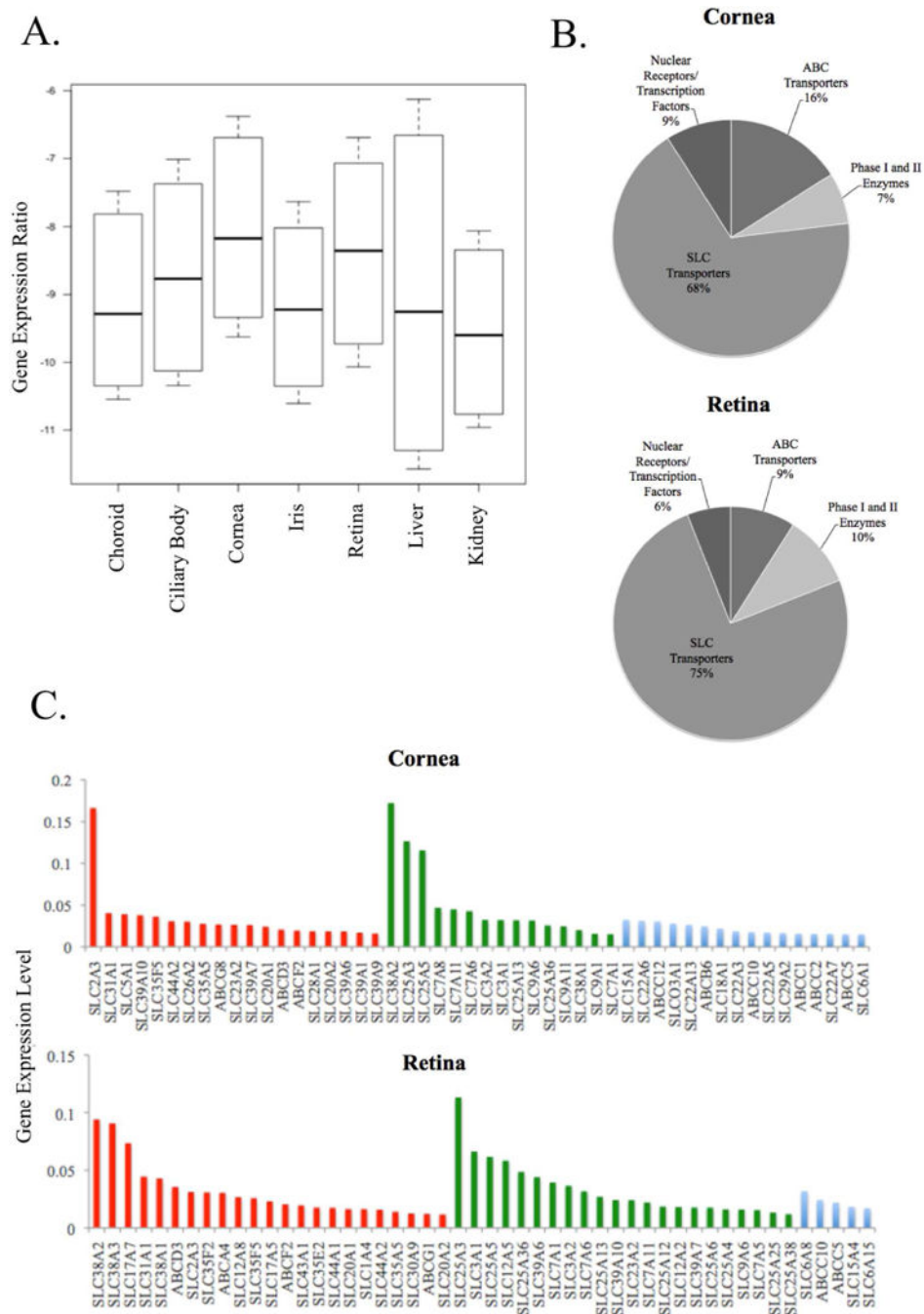


Figure 1. Analysis of Array Gene Expression

The distribution of mRNA expression values (log-transformed Ct values) for all genes in all eye regions (n=15) in addition to the liver (n=60) and kidney (n=60) is shown in the boxplot (A). Ocular data are from six orbs obtained from three individuals, see Supplemental Table S1 for donor information. The boxes depict the 25th and 75th percentile (the lower and upper quartiles, respectively), the middle band is the 50th percentile (median) and the upper and lower whiskers represent the data minimum and maximum, respectively. (B) The pie graphs show the distribution of functional annotation categories (SLC

transporters, ABC transporters, Phase I and Phase II enzymes, nuclear receptors and transcription factors) of the top-100 most highly expressed genes in the cornea (top graph) and retina (bottom graph). (C) Bar graphs of the top 50 most highly expressed transporter genes, separated into three functional classes, are shown for the cornea (top plot) and retina (bottom plot). On the y-axis, Ct levels for each gene are shown, while the colored bars on the x-axis correspond to annotated functional class: nutrient transporters (red), xenobiotic transporters (blue) and other molecular or functional role (green).

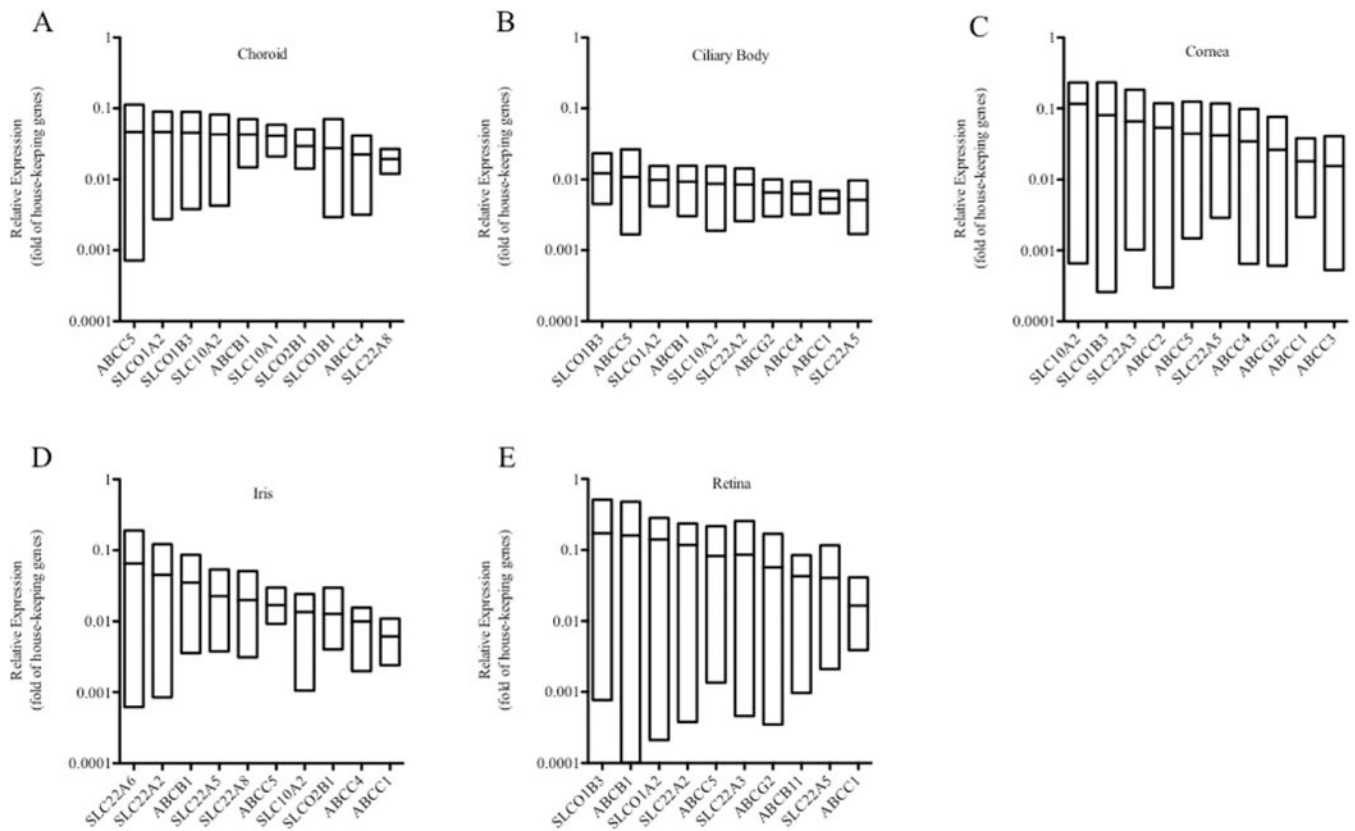


Figure 2. Relative Gene Expression in Different Eye Regions

The ten most highly expressed TransPortal genes in each region of the human eye are shown: choroid (A), ciliary body (B), cornea (C), iris (D), and retina (E). Data are from six orbs obtained from three individuals, see Supplemental Table S1 for donor information. Each data point corresponds to one donor, with RNA from each region of both orbs used to measure expression. Expression values of all genes are presented as fold difference relative to the mean of housekeeping genes within each sample. Only genes detected in at least two donors were included. For each gene, the upper and lower limit of each box represents the highest and lowest expression value, respectively, and the middle line within each box represents the mean expression value.

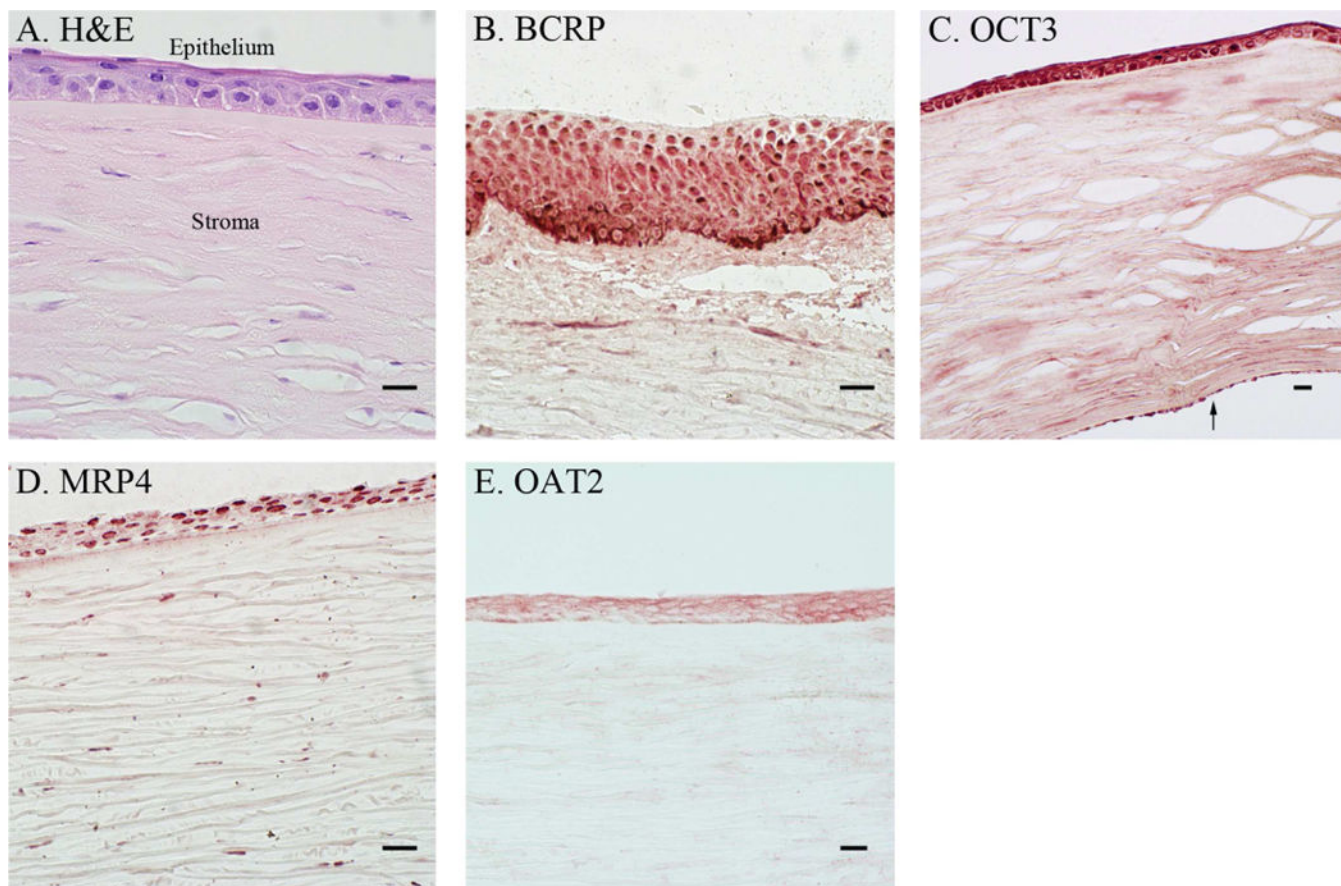


Figure 3. Immunohistochemical Analysis of Transporter Gene Expression in the Cornea
Control cornea sections were prepared with hematoxylin-eosin (H & E) staining (A) to differentiate the tissue layers (epithelium and stroma are labeled). Protein expression pattern of four transporters was evaluated by IHC: BCRP (B), OCT3 (C), MRP4 (D), and OAT2 (E). In (C) the arrow (↑) denotes the corneal endothelium. Scale bars are set to 20 microns. Data are from three orbs obtained from two individuals, see Supplemental Table S1 for donor information. An eye pathologist reviewed all IHC of the cornea.

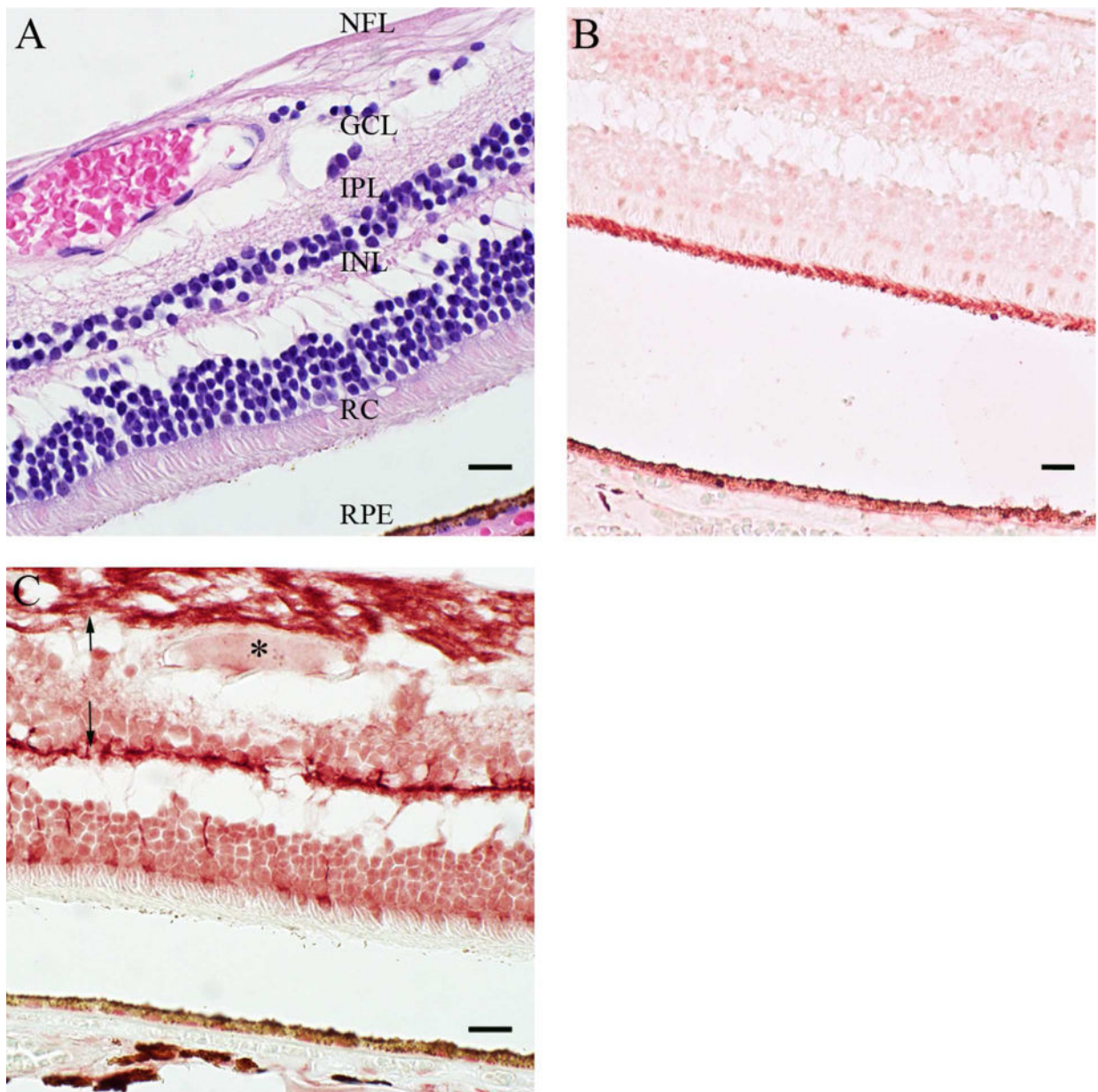


Figure 4. Immunohistochemical Analysis of Transporter Gene Expression in the Retina
 Control retina sections were prepared with hematoxylin-eosin (H & E) staining (A) to differentiate the tissue layers. The protein expression pattern of two transporters was evaluated by IHC: OCT3 (B) and BCRP (C). (C) The arrow (↑) and the asterisk (*) denote nerve fibers and a blood vessel, respectively. Scale bars are set to 20 microns. See Supplemental Table S1 for donor information. An eye pathologist reviewed all IHC of the retina. RPE, retinal pigmented epithelium; RC, rods and cones; INL, inner nuclear layer; IPL, inner plexiform layer; GCL, ganglion cell layer; NFL, nerve fiber layer.

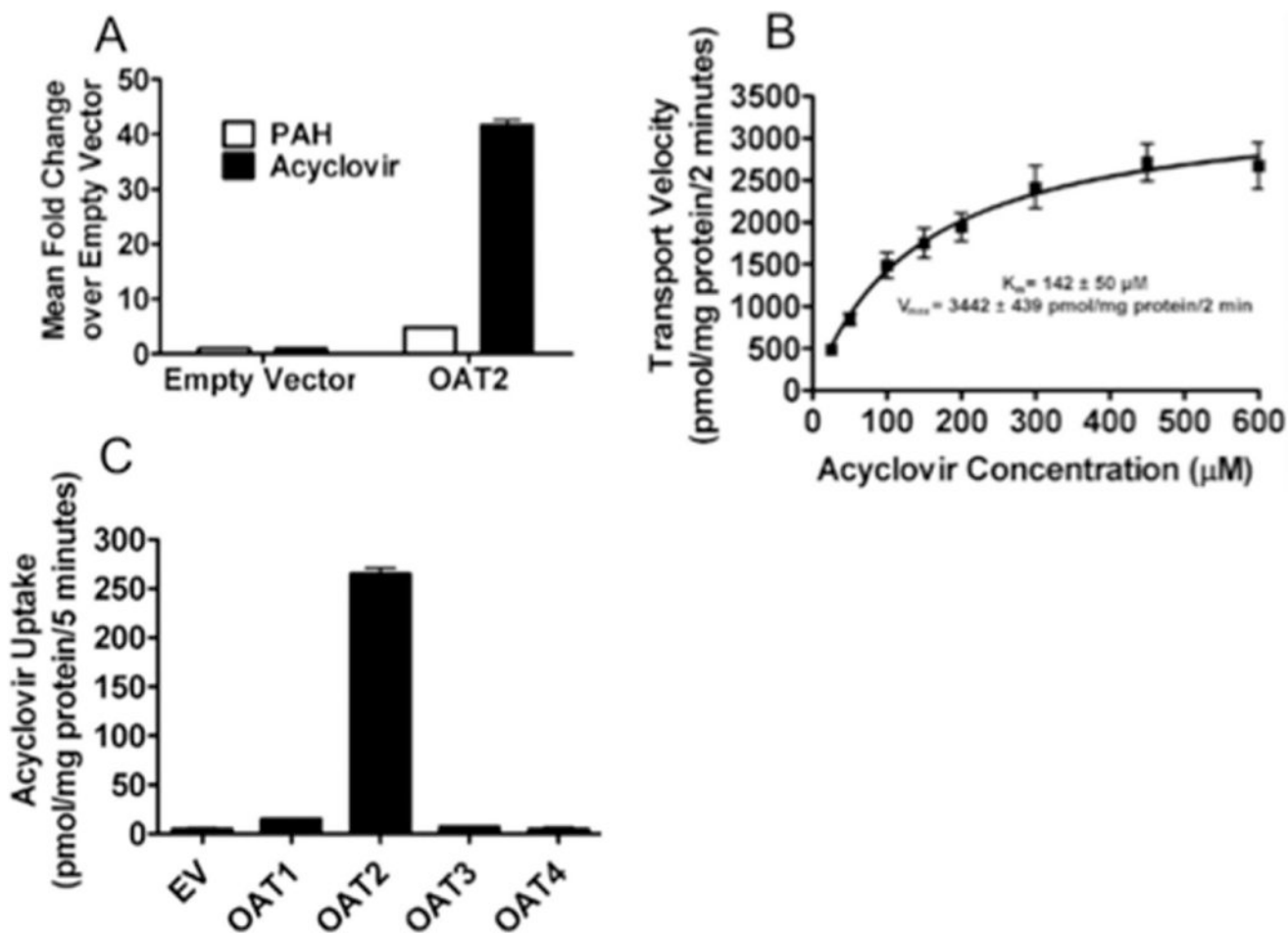


Figure 5. Transport of Acyclovir by hOAT2-HEK293 Cells

The uptake kinetics of [^3H]-acyclovir were evaluated in OAT2-transfected HEK293 cell lines using a 2 minute incubation period. Uptake of [^3H]-acyclovir was substantially greater than that of [^3H]-PAH in the OAT2 expressing cells, but not the control (empty vector) cells (A). The kinetics of OAT2-HEK293 cell mediated transport of [^3H]-acyclovir transport was high-capacity and moderate affinity (B). Acyclovir uptake was greatest in cells expressing OAT2 in comparison to cells expressing OAT1, OAT3 or OAT4 under the same experimental conditions (C). Values represent mean \pm SEM of at least three replicate determinations in a single experiment.

Table 1
Primary antibodies used in immunohistochemistry

Target Protein	Titer	Source
BCRP	1:50	Alexis, Farmingdale, NY
MRP1	1:50	Alexis, Farmingdale, NY
MRP2	1:50	Genway, San Diego, CA
MRP4	1:20	Alexis, Farmingdale, NY
MRP5	1:50	Alexis, Farmingdale, NY
OCT3	1:100	Abcam, Cambridge, MA
OCT3	1:100	GenWay Biotech, San Diego, CA
OAT2	1:450	Sigma Aldrich, St. Louis, MO
OATP1B3	1:350	Sigma-Aldrich, St Louis, MO

Table 2
The localization of various ocular membrane transporters and their ocular drug substrates

Gene	Protein Name	Ocular Drugs	Route of Administration	Transport		Localization		References
				Direction*	Mechanism	Previous Study	Current Study	
SLC15A1	PEPT1	amoxicillin, valacyclovir	topical, oral	Absorptive	H ⁺ -coupled symporter	iris, ciliary body, cornea	choroid, cornea, retina	[30, 66-68]
SLC15A2	PEPT2	amoxicillin	topical	Absorptive	H ⁺ -coupled symporter	cornea, retina, choroid, ciliary body, iris	none	[30, 66]
SLC22A1	OCT1	ganciclovir, acyclovir, atropine	topical, systemic	Absorptive	Electrogenic, Na ⁺ -independent	cornea, retina, choroid, iris, ciliary body	choroid, cornea	[30, 69, 70]
SLC22A2	OCT2	acyclovir, ganciclovir, atropine, epinephrine	topical, systemic	Absorptive	Electrogenic, Na ⁺ -independent	iris, ciliary body	choroid, ciliary body, cornea, iris, retina	[30, 69-72]
SLC22A3	OCT3	verapamil, bromonidine, atropine, epinephrine	topical	Absorptive	Electrogenic, Na ⁺ -independent	cornea, retina, choroid, iris, ciliary body	choroid, ciliary body, cornea, iris, retina	[30, 69, 72, 73]
SLC22A4	OCTN1	verapamil	topical	Absorptive	Electrogenic, Na ⁺ -independent	cornea, retina, choroid, iris, ciliary body	none	[30, 74]
SLC22A5	OCTN2	verapamil	topical	Absorptive	Electrogenic, Na ⁺ -independent	cornea, retina, choroid, iris, ciliary body	choroid, ciliary body, cornea, iris, retina	[30, 75]
SLC22A6	OAT1	cefazolin, penicillin G, tetracycline, acyclovir, cidofovir, ganciclovir, zidovudine	topical, oral, systemic	Absorptive	Organic anion/dicarboxylic acid exchanger	retina, iris, ciliary body	choroid, cornea, iris	[30, 70, 76-80]
SLC22A7	OAT2	acyclovir, cefazolin, penicillin G, tetracycline, erythromycin, zidovudine, 5-fluorouracil	topical, oral, systemic	Absorptive	Organic anion/dicarboxylic acid exchanger	none	cornea	[30, 70, 81-83]
SLC22A8	OAT3	cefazolin, penicillin G, tetracycline, acyclovir, valacyclovir, zidovudine	topical, oral, systemic	Absorptive	Organic anion/dicarboxylic acid exchanger	retina, choroid, iris, ciliary body	choroid, cornea, iris	[27, 30, 70, 76, 81]
SLC22A11	OAT4	cefazolin, penicillin G, zidovudine, diclofenac, tetracycline	topical, oral	Absorptive	Organic anion/dicarboxylic acid exchanger	ND	none	[70, 76, 81]
SLC22A12	URAT1	unknown				ND	none	
SLC47A1	MATE1	ganciclovir, acyclovir	topical, systemic	Absorptive/Secretive	H ⁺ -coupled antiporter	ND	iris	[84]
SLC47A2	MATE2	ganciclovir, acyclovir	topical, systemic	Absorptive/Secretive	H ⁺ -coupled antiporter	ND	cornea	[84]
SLC01A2	OATP1A2	dexamethasone, erythromycin, levofloxacin	topical	Absorptive	Na ⁺ -independent exchanger	retina, choroid	choroid, ciliary body, iris, retina	[30, 85, 86]
SLC10A1	NTCP	unknown				ND	choroid, ciliary body, cornea	
SLC10A2	ASBT	unknown				none	choroid, iris, ciliary body, cornea, retina	
SLC01B1	OATP1B1	unknown				none	choroid, ciliary body, cornea, iris	
SLC01B3	OATP1B3	Cyclosporine A, penicillin G	topical, systemic	Absorptive	Na ⁺ -independent exchanger	retina	choroid, ciliary body, retina, cornea, iris	[87]
SLC02B1	OATP2B1	Cyclosporine A	topical	Absorptive	Na ⁺ -independent exchanger	cornea, retina, choroid, iris, ciliary body	choroid, ciliary body, cornea, iris	[30, 86, 88]
ABCB1	MDR1/P-gp	Cyclosporine A, erythromycin, acebutolol, timolol, levofloxacin, miconazole, dexamethasone, hydrocortisone, prednisolone, verapamil	topical, oral	Secretive/Efflux	ATP-dependent efflux pump	cornea, retina, choroid, iris, ciliary body	choroid, iris, ciliary body, retina, cornea	[27, 30, 89-95]
ABCB11	BSEP	unknown				ND	choroid, ciliary body, cornea, retina	
ABCB4	MDR2	verapamil	topical	Secretive/Efflux	ATP-dependent efflux pump	ND	ciliary body, cornea	[96]
ABCC1	MRP1	glutathione and glutathione conjugates, leukorriene C4, estradiol-17-beta-o-glucuronide, erythromycin, clotrimazole	topical	Secretive/Efflux	ATP-dependent efflux pump	cornea, retina, choroid, iris, ciliary body	iris, ciliary body, retina, cornea	[30, 89, 90]
ABCC2	MRP2	erythromycin, acyclovir	topical, systemic	Secretive/Efflux	ATP-dependent efflux pump	retina, choroid	choroid, cornea	[30, 89, 90, 93, 97, 98]
ABCC3	MRP3	unknown				cornea, retina, choroid, ciliary body, iris	cornea	[89, 90]
ABCC4	MRP4	ganciclovir, zidovudine	topical, oral	Secretive/Efflux	ATP-dependent efflux pump	ND	choroid, iris, ciliary body, cornea, retina	[89, 90]

Gene	Protein Name	Ocular Drugs	Route of Administration	Transport		Localization		References
				Direction *	Mechanism	Previous Study	Current Study	
ABCC5	MRF5	bimatoprost, latanoprost, acyclovir, 5-fluorouracil	topical, systemic	Secretive/Efflux	ATP-dependent e flux pump	cornea, retina	choroid, iris, ciliary body, retina, cornea	[89, 90, 98, 99]
ABCC6	ARA	unknown				ND	cornea	
ABCG2	BCRP	acyclovir, cyclosporine, ciprofloxacin, norfloxacin, ofloxacin, zidovudine, dexamethasone, trinitroton	topical, systemic, oral	Secretive/Efflux	ATP-dependent e flux pump	cornea, retina, ciliary body, iris, choroid	ciliary body, retina, cornea, choroid	[30, 89, 90, 100]

ND, not determined.

* SLC transporters can function bidirectionally; therefore direction depends on the chemical gradient of the substrate and where applicable the gradient of the co-transported or counter-transported ion.